Thermo-acoustic performance of green roof substrates in dynamic hygrothermal conditions

Claudia Fabiani[a], Julià Coma[b], Anna Laura Pisello[a,c], Gabriel Perez[d], Franco Cotana[a,c], Luisa F. Cabeza[d,*]

[a] *CIRIAF – Interuniversity Research Center on Pollution and Environment "Mauro Felli", Via Duranti 67, 06125 Perugia, Italy.*

[b] *Department de Tecnologia de l'Arquitectura, Universitat Politècnica de Catalunya, Av. Dr. Marañón 44-50, Barcelona, Spain.*

[c] *Department of Engineering – University of Perugia, Via Duranti 63, 06125 Perugia, Italy.*

[d] *GREiA Research Group, INSPIRES Research Centre, Universitat de Lleida, Pere de Cabrera s/n, Lleida, Spain.*

**Corresponding author: lcabeza@diei.udl.cat*

Abstract

Green roofs can be considered as effective and esthetically appreciated passive tools for energy saving systems in buildings. In particular, the effect of evapotranspiration and the large thermal inertia of such solutions, represent highly attractive properties to be implemented in advanced building envelope components. Although these properties are deeply influenced by external factors such as weather conditions, and greenery dynamics, the materials used in substrate and drainage layers are too commonly assumed as constant thermal insulation layers depending only on their physical properties and water content. In particular, common disaggregated materials used in internal layers of extensive green roofs, generally are characterized by a highly complex matrix, and consequently, such materials usually lack of realistic thermal-acoustic properties evaluation. The main objective of the study is to investigate the impact of water content on the thermo-acoustic performance of different disaggregated materials from green roofs substrates commonly used in Mediterranean climates. In particular, the TPS method was used to assess the effect of humidification and raining processes on the final performance of the considered samples. An extensive acoustic characterization was also developed, based on the acoustic transfer function method. Results show that raining processes can highly influence the thermal performance of such materials, which depending on their density, can even triple their thermal conductivity value and achieve twice the volumetric specific heat at ambient conditions. Furthermore, the acoustic characterization procedure showed that the biggest modification on the final acoustic absorption and insulation capability, i.e. about 20 dB when the 80 mm samples, was produced by increasing the water content of the system from 10% to 30% RH. On the contrary, the conditioning at 90% RH does not produce significant differences of the final acoustic behavior of the substrates.

Keywords: green roofs, substrates, dynamic conditions, thermal insulation; acoustic absorption and insulation; energy efficiency in buildings; passive cooling.

NOMENCLATURE

R(t)	Resistance of the Hot Disk probe [Ω].
R_0	Initial resistance of the Hot Disk sensor [Ω].
P_0	Power supplied during the Hot Disk measurement [W].
a	Hot Disk temperature coefficient of resistivity (TCR) [1/K].

ΔTi	Temperature difference across the insulating layers of the Hot Disk probe [K].
$D(\tau)$	Dimensionless shape function [-].
τ	Dimensionless time [-].
K	Thermal diffusivity [mm^2s^{-1}].
k	Thermal conductivity [$Wm^{-1}K^{-1}$].
ρ	Density [kgm^{-3}].
ρc_p	Volumetric specific heat [$MJm^{-3}K^{-1}$].
α	Acoustic absorption coefficient [-].
TL	Acoustic transmission loss [dB].
T_{air}	Air temperature [C].
$T_{Sol-air}$	Sol-air temperature [C].
α_{rad}	Solar absorption coefficient [-].
I_g	Global solar radiation and the horizontal plane [Wm^{-2}].
R_{se}	External surface resistance [m^2KW^{-1}].
RH	Relative humidity [-]

1. Introduction

Energy efficiency in buildings represents a key research and industrial issue to be addressed all around the world, since buildings require more than 35-40% of final energy uses in developed countries [1]. In this view, a variety of new calculation tools and technologies, building integrated renewables and high-performance materials are under development by the scientific and real market world nowadays [1]-[4]. More in detail, several envelope materials [5],[6] and whole solutions [7]-[9] showed interesting potentialities also in mitigating urban overheating and, more in general, in improving urban quality of life from thermal, acoustic, and visual comfort perspective in the built environment. Among such solutions green roofs probably represent the most widely acknowledged and investigated bioclimatic approach [10]-[14].

This kind of application is typically designed for improving roof thermal insulation performance in winter conditions, while taking advantage of evapotranspiration processes during summer, thus globally reducing the final thermal energy consumption of the building [15],[16]. Given their thermo-physical characteristics, green roof solutions also allow to enhance roofs thermal inertia, protect and preserve the functionality of waterproof membranes, and buffer storm water runoff [17],[18]. Additionally, the implementation of vegetated roofs and walls in buildings has also been proved to provide the building envelope with advanced acoustic absorption and insulation capability [19]-[23] and they can take advantage of recycled sustainable materials and components [21]. Finally, green roofs applications are also widely appreciated for esthetic and architectural motivations [24]-[26].

From the thermal-energy point of view, green roof applications are mostly affected to three basic phenomena: (i) the combined insulation-thermal energy storage effect due to the green roof draining layer, (ii) the shadow effect produced by the vegetation above it, and (iii) the evapotranspiration phenomenon occurring in both of them [26]-[28]. The former effect is directly related to a set of physical properties such as layer thickness, density, thermal conductivity, and specific heat, while the second one is mainly related to the kind of plant selected for the specific green roof application, mostly in terms of leaf area index (LAI) and plant cover. Finally, the latter phenomenon, which can reduce the heat island effect by humidifying and consequently cooling the outdoor environment, is basically affected by the ground water content [16],[29].

From the acoustic perspective, the insulation capability of the vegetated roof is generally recognized to be a function of the growing substrate thickness and density [23], while the acoustic absorption coefficient is mostly affected by the organic content, and by the ground compaction level [22]. Additionally, both properties seem to be somehow influenced by the water content in the substrate itself [30].

Despite the huge investigation around this topic, several assumptions are still made when the green roof thermal-energy, and acoustic performance is assessed and the dynamic behavior of permeable green roof components is frequently underestimated or, at least, would deserve a better attention while elaborating dynamic reliable prediction models [3],[31],[32]. Green roof multilayer structures generally include stone or ground based aggregates, sand and/or organic matter acting as substrate for water draining and plant nutrition storage. Mainly, natural soils are used as substrates for these applications, in fact, several research contributions focusing on the thermal properties of this kind of materials can be found in the literature [33],[34]. However, in most cases, these substrates have been characterized in dry conditions, representing summer non-rainy weather in Mediterranean area [17].

This work focuses on the investigation of the thermal and acoustic performance of typical green roof substrates under varying hygrothermal conditions. The proposed experimental procedure aims at investigating the influence of water content on the thermal and acoustic properties of the investigated samples, by coupling advanced thermal-acoustic analyses and a controlled environment. More in detail, five substrates for extensive green roof applications, characterized by different organic content and density values, were selected and exposed to a representative relative humidity fluctuation. Additionally, a raining process was also simulated and the effect of the following natural drying path on the final thermal behavior of the samples was assessed.

2. Materials and methodology

2.1. Materials

In this work, the thermal-acoustic behavior of engineered substrates with different density and composition was experimentally evaluated as a function of their water content. The selection of five substrates (Figure 1),

specifically developed for green roof applications, was based on the aim to analyze different suitable compositions for the Mediterranean climate conditions, which are characterized by huge oscillations in relative humidity during most of the year, experiencing precipitations during winter, autumn, and spring, but also thunderstorm and heavy rainfalls during the hot-dry summer.

All this considered, substrates with relatively low bulk density, capable to retain sufficient water for plant growth, but also to allow free draining when exposed to heavy rain falls were selected. Moreover, these samples were also chosen in order to be representative of a wide range of natural substrates produced by introducing variable quantities of crushed building wastes in the original soil matrix. In particular, densities between 0.375 and 0.923 g/cm^3 were considered, with an organic content ranging between 6.773 and 14.107% of the final weight of the substrate. Furthermore, an additional soil mix, i.e. Substrate 5 in Figure 1, produced without using any recycled material from crushed building wastes and characterized by a 40% in weight of organic material was also analyzed. The composition of the considered materials and their relevant physical characteristics are shown in Table 1.

Figure 1. Analyzed green roof substrates.

Table 1. Composition of the analyzed green roof substrates.

SAMPLE	COCO PEAT (vol.%)	COMPOST (vol.%)	CRUSHED BUILDING WASTES (vol.%)	COARSE GRAINED SAND (vol.%)	ORGANIC CONTENT (wt.%)*	MINERAL CONTENT (wt.%)	DENSITY WHEN DRY (g/cm^3)*
SUBSTRATE 1	25	25	40	10	6.773	(n.a.)	0.923
SUBSTRATE 2	25	40	30	5	14.107	(n.a.)	0.546
SUBSTRATE 3	60	15	20	5	12.579	(n.a.)	0.375
SUBSTRATE 4	25	45	20	10	11.189	(n.a.)	0.582
SUBSTRATE 5	(n.a.)	(n.a.)	(n.a.)	(n.a.)	40	60	0.696

*Given by the company

2.2. Methodology for assessing thermal properties

The overall thermal characterization of the samples was carried out using a Hot Disk 2500S equipment and according to the ISO 22007-2 standard [35]. The Hot Disk makes use of the Transient Plane Source (TPS) method, which allows performing accurate thermal conductivity and thermal diffusivity measurements while also enabling to evaluate the specific heat of the tested sample from one single transient recording [36]. In

the basic principle of the TPS method, a planar 10 μm thick double Nickel spiral is sandwiched between two identical samples of the same material and provides them with a certain heating power P_0 for a specific amount of time t. During this time interval, the resistance of the probe R(t) is continuously monitored and finally related to thermal properties of the bulk material by using Equation (1):

$$R\,(t) = R_0 \left\{1 + a\left[\Delta T_i + \frac{P_0}{\pi^{2/3} rk} D(\tau)\right]\right\} \quad (1)$$

where t is the test time [s], R_0 is the initial resistance of the sensor at time t=0 [Ω], a is the temperature coefficient of resistivity (TCR) [1/K], ΔT_i is the temperature difference across the insulating layers of the probe [K], D(τ) is the dimensionless shape function and τ is the dimensionless time, which is a function of sample's thermal diffusivity (K).

In Equation (1), R(t) increases linearly with D(τ), in fact, the factor $R_0(1 + a\Delta T_i)$ varies with the same trend of ΔT_i, while $\left(aR_0P_0/\pi^{3/2}rk\right)$ is a constant for an established measurement system. Such linear relation can be established by a least-squares fitting and finally thermal conductivity can be obtained through a process of iteration. Furthermore, the relation between thermal conductivity and thermal diffusivity of the tested material, can also be used to determine its specific heat:

$$k = \mathrm{K} \cdot \rho c_p \quad (2)$$

where ρ is the density and c_p is the specific heat of the sample.

2.3. Methodology for assessing acoustic properties

The acoustic characterization of the samples was carried out both in terms of sound absorption and sound insulation properties, by means of an impedance tube (Kundt's tube). Such properties where defined measuring the normal incidence absorption coefficient (α) and the transmission loss (TL) of the considered samples. The absorption coefficient can be described as the percentage of the incident sound wave acoustic energy that is not absorbed by the tested sample and it is experimentally determined by means of the so-called Transfer Function Method (TFM), according to the ISO 10534-2 standard [29]. In the TFM, plane waves are generated in a tube by a noise source and the decomposition of the interference field in (i) an incident plane wave (generated by the noise source), and (ii) a reflected plane wave (by the material) is achieved by measuring the acoustic pressure at two fixed locations (using wall-mounted microphones), and by calculating the complex acoustic transfer function and consequently the normal incidence absorption of the acoustic material.

The second parameter that was analyzed by means of the impedance tube is the transmission loss, which on the other hand, is a key factor for the quantification of the insulation properties of an acoustic material. This parameter is related to the sound transmission coefficient (τ_s) by the:

$$TL = 10 \cdot log\left(1/\tau_s\right) \quad (3)$$

It is measured by means of the 'two-load' transfer function method [38],[39], acquiring the sound pressure in four fixed microphone positions and it can be considered as an extension to four microphones of the previously explained TFM. As in the previous case, this approach assumes that the sound field in the up and downstream segments of the standing wave tube, can be well approximated by superposition of positive and negative-directed plane waves. The main difference with the previous analysis lies in the fact that this time the measurement is repeated with two configurations of the tube termination, i.e. anechoic and rigid.

2.4. Dynamic assessment of the selected thermo-acoustic properties

The main purpose of this work is to evaluate the effect of realistic relative humidity fluctuations on the thermo-acoustic behavior of the extensive green roof substrates described in Section 2.1. Two experimental equipment were used to carry out the thermo-acoustic analyses: the Hot Disk 2500S and the Brüel & Kjær 4260 impedance tube. These appliances were specifically selected and used during the experimental campaign for three different reasons: (i) they allow to investigate the desired thermo-acoustic properties by means of rapid and simple measurements, (ii) they make use of small samples which can also be made of disaggregated materials and (iii) their experimental technique can be combined with an environmental conditioning procedure, to perfectly control temperature and relative humidity conditions during the measurement. As a matter of fact, and as described in Section 2.2, the Hot Disk apparatus relies on a transient experimental procedure, which conversely to common steady-state techniques such as the guarded hot-plate (GHP) and the heat flow meter (HFM), evaluates the feedback response of the specimen after a heating signal is transmitted to it during a short transient. Consequently, Hot Disk measurements are relatively quick and need samples of a few centimeters to produce reliable results.

Similarly, the impedance tube relies on a controlled plane waves acoustic field to investigate the acoustic performance of relatively small samples by rapidly modifying the wavelength of the sound wave impinging on their surface. Also in this case, due to physical and geometrical reasons the measurement is faster than similar analyses carried out using reverberant chambers or similar equipment, which by the way, also need complex and expensive experimental setups.

In order to investigate the sample's reaction varying humidity values under a daily basis, real meteorological data from a weather station located on the rooftop of Perugia University (Italy) were considered. More in detail, the weather data from January 1st to July 31st 2017 were analyzed, and the day with the highest diurnal oscillation in the relative humidity values, i.e. April 8th, was selected to be reproduced in the simulated environment of a climatic chamber (Figure 2).

As seen in Figure 2, the huge relative humidity variation takes place in the time interval between 4:30 am and 11:30 am, (the green area in the graph). These specific environmental conditions were selected and reproduced within the controlled environment of a climatic chamber to investigate the performance of the different samples under extreme humidity variations. Furthermore, given the pseudo linear trend registered in

the selected time interval, and the precision of the climatic chamber in controlling humidity, i.e. ±3% RH, a simple linear ramp between 30 and 90 % RH was considered in the experimental campaign, together with two steady state segments before and after the ramp itself (for further details see Section 3.1). Lastly, since the Hot Disk and the original TPS method can only be applied when the investigated sample is in steady-state temperature conditions, an average temperature value is defined for conditioning the samples, i.e. 21°C. The temperature forcing in the hygrothermal cycles was defined by considering the average value of the sol-air temperature for a horizontal stratigraphy exposed to the selected weather conditions. The sol-air temperature ($T_{Sol-Air}$) was computed according to Equation (4) 23[40]:

$$T_{Sol-air} = T_{air} + \alpha_{rad}\, I_g R_{se} \quad (4)$$

where T_{air} is the outdoor air temperature from the weather file [C]; α_{rad} is the solar absorption coefficient of the substrates; I_g is the global solar radiation also from the weather file [Wm^{-2}]; and R_{se} is the external surface resistance [m^2KW^{-1}]. An absorption coefficient α_{rad} equal to 0.6 and an external surface resistance R_{se} equal to 0.04 m^2KW^{-1} were considered for the substrates, in accordance to the recommendations of ISO 6946 [41].

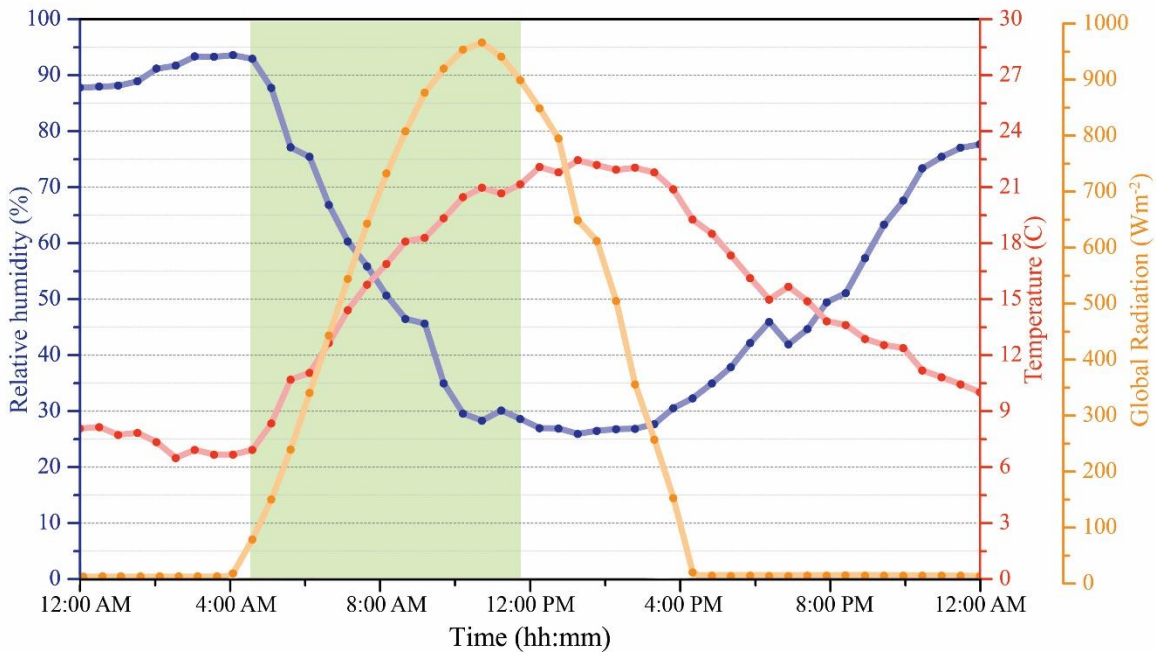

Figure 2. Relative humidity, air temperature and global radiation values registered by the weather station at Perugia University on April 8th 2017.

3. Thermal and acoustic analysis

3.1. Experimental campaign for thermal characterization

The thermal characterization of the samples was carried out by means of a Hot Disk 2500S apparatus with using a 4922 sensor (14.6 mm). The different grains were measured by using as a sample holder a cylindrical

plastic container with a narrow horizontal opening in the center of the lateral surface (Figure 3). A first layer of grains of about 4 cm was placed inside the sample holder, then the hot disk sensor was introduced in the narrow opening and located in a planar position upon the grains. Lastly, the probe was completely covered by a second layer of grains with a uniform thickness of about 4 cm.

In order to analyze the variation of the parameters describing the thermal behavior of the samples with respect to their water content, the transient analysis was carried out within the test compartment (601×810×694 mm^3) of an ATT DM340SR climatic chamber, which can guarantee a temperature and humidity-controlled environment in the range -40÷180°C ±1°C and 10÷98% ±3% of RH. Each sample was conditioned by means of three different hygrothermal cycles, i.e. (i) 10% RH cycle, (ii) 30 → 90% RH cycle, and (iii) 90 → 30% RH cycle; which are described in further detail in Table 2.

Cycle (i) was designed in order to investigate the performance of the selected substrates at the average temperature obtained from the weather data in Section 2.4, considering extremely dry conditions, i.e. 10%. Cycle (ii) and (iii), on the other hand, were designed to directly reproduce the selected environmental conditions and analyze the effect of water content on the effective thermal properties of the samples, considering an increasing and a decreasing humidity ramp, respectively.

In cycle (iii), the grains were saturated with the addition of 250 g of water, i.e. between 1/3 and 1/4 of the total weight of the investigated soil, before being introduced in the controlled environment of the climatic chamber. During (ii) and (iii) cycles the thermal properties of each sample were tested every 30 minutes in the schedule mode of operation of the hot disk apparatus. The thermal properties in dry conditions were instead evaluated only during the last hour of the second step of cycle (i) (1 measurement every 30 minutes), and the average value was calculated.

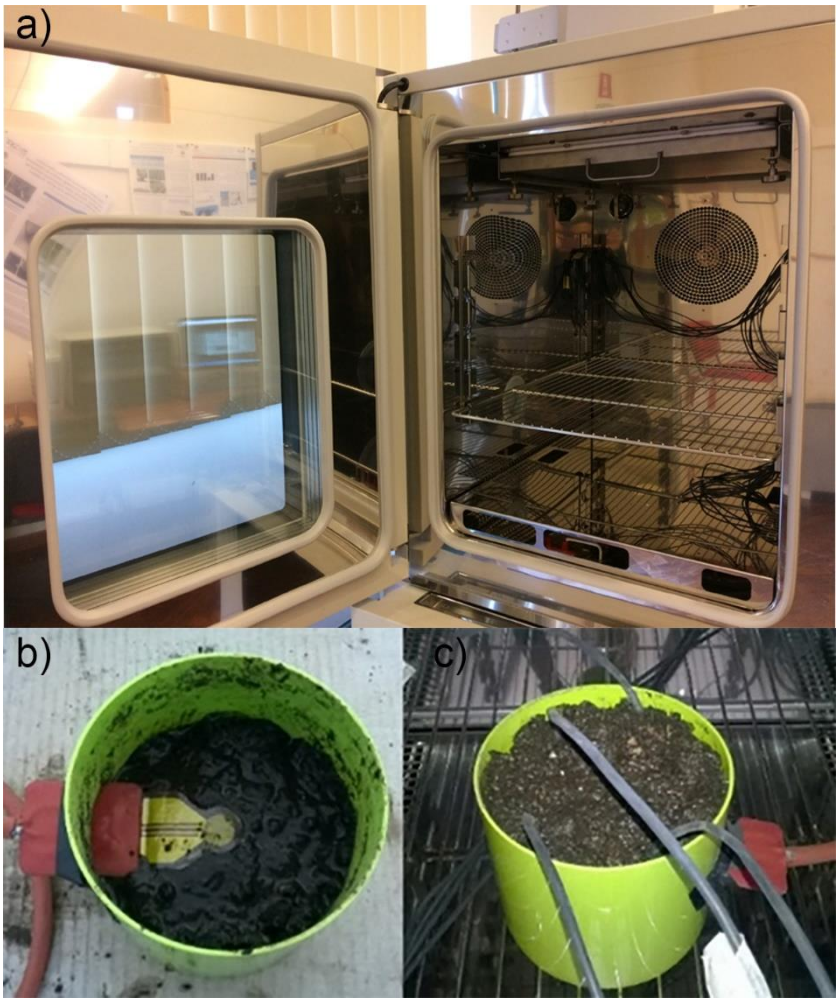

Figure 3. (a) Internal compartment of the climatic chamber; (b) First layer of grains with TPS sensor; (c) final experimental setup.

Table 2. Hygrothermal cycles simulated in the environmental chamber.

(i)	STEP	STEP 1	STEP 2	
	Temperature set point	70°C	21°C	
10% RH	RH set point	10%	10%	
cycle	Duration	10 hours	5 hours	
(ii)	STEP	STEP 1	STEP 2	STEP 3
	Temperature set point	21°C	21°C	21°C
30→90%	RH set point	30%	30→90%	90%
RH cycle	Duration	3 hours	7 hours	3 hours
(iii)	STEP	STEP 1	STEP 2	STEP 3
	Temperature set point	21°C	21°C	21°C
90→30%	RH set point	90%	90→30%	30%
RH cycle	Duration	3 hours	7 hours	3 hours

3.2. Experimental campaign for acoustic characterization

The acoustic characterization of the grains was carried out in terms of both absorption coefficient and transmission loss by means of an impedance tube (Brüel & Kjær, model 4260), using a two (α) and a four microphones method (TL), respectively. Both parameters were evaluated for four different thickness of the samples, i.e. 20, 40, 60 and 80 mm, at the end of the last step of the thermal cycle (i), i.e. at an RH value of

about 10%, and at the end of the first and the final step of cycle (ii), i.e. at an RH value of about 30 and 90%, respectively.

The absorption coefficient measurements were carried out by performing the following steps:

- atmospheric pressure, air temperature, and relative humidity were measured and used to define the environmental boundary conditions;
- microphones calibration was accomplished;
- the samples were placed inside the sample holder; and
- signal-to-noise ratio and transfer function calibration for the channels phase displacements were evaluated.

The measurements of the Transmission Loss were carried out with the two-load method, through the following main steps:

- atmospheric pressure, air temperature, and relative humidity were measured and used to define the environmental boundary conditions;
- background noise calibration measurement was performed with an anechoic and a rigid termination of the tube;
- the samples were introduced in the sample holder; and
- signal measurements were completed with both the anechoic and the empty end of the tube.

All the measures to determine the absorption coefficient and the Transmission Loss were carried out using both the large tube (sample diameter 100 mm) and the small tube configuration (sample diameter 29 mm), in order to cover the range of frequencies between 50 and 6400 Hz for all the considered samples.

4. Results and discussion

4.1. Results from the thermal characterization

Results from the thermal analysis carried out during cycle (i) are reported in Figure 4. As can be seen, in simple dry conditions the substrates show relatively low thermal conductivities and diffusivities (always below 0.311 W/(m·K) and 0.493 mm/s^2), furthermore, the highest and the lowest values of such properties are always associated to the substrates with the lowest and the biggest organic content, i.e. substrate 1 and 5 characterized by a 6.773 and 40% of organic matter on the final weight of the sample, respectively. In addition, it can be stated that even though largely influenced by the density of the samples, the volumetric specific heat is also highly related to the overall organic content of the composite soil. In fact, the lowest $\rho \cdot c_p$ values, i.e. 0.508 ± 0.036 MJ/(m^3·K) and 0.504 ± 0.019 MJ/(m^3·K), are associated to Substrate 3 and 5 that possess the lowest density among the samples with a comparable organic content, and the highest organic content among the samples with comparable density, respectively.

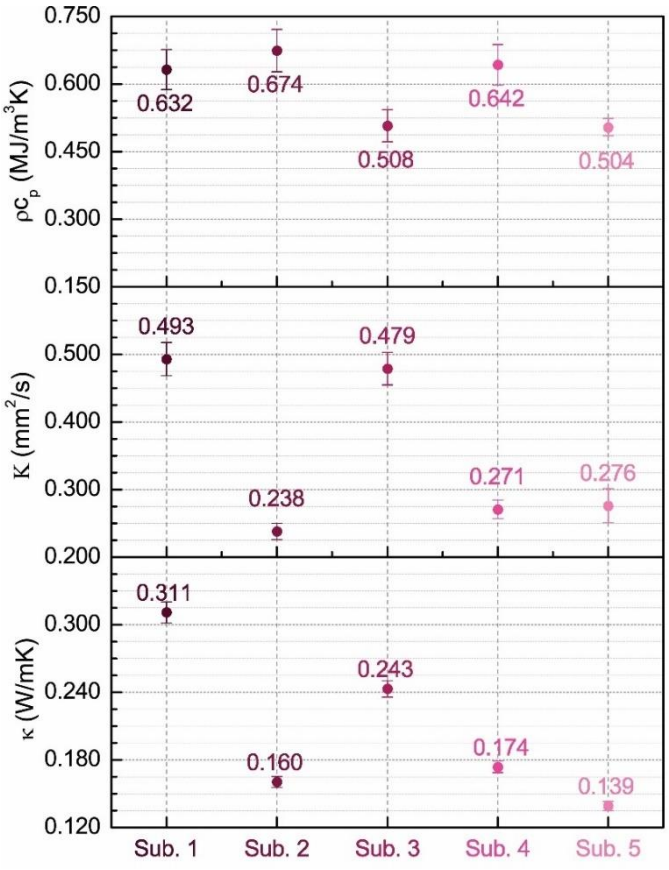

Figure 4. Thermal analysis at 21°C and 10% RH.

During cycle (ii), characterized by an increasing relative humidity transient step, i.e. from 30% RH to 90% RH, the samples maintain similar thermal properties in comparison to the previous analysis, although all of them experience a comparable variation trend while increasing their relative humidity to 30%, i.e. at the beginning of cycle (ii). As a matter of fact, and as expected, in the transition from extra dry conditions to about 30% RH every sample enhances its thermal conductivity and volumetric specific heat, while their thermal diffusivity is lowered (Figure 5a). To better understand this variation, it must be noticed that before running the cycle, the substrates were stored at ambient conditions, around 30% RH and 20°C for several days. In any case, as seen in Figure 6, none of the samples were highly influenced by the imposed hygrothermal forcing during the 13 hours-long cycle, since all the experienced variations were negligible within the experimental error of the TPS measurement. This would suggest that the thermal behavior of the substrates is not seriously affected by the diurnal oscillations even when extremely variable forcing conditions are imposed for several hours.

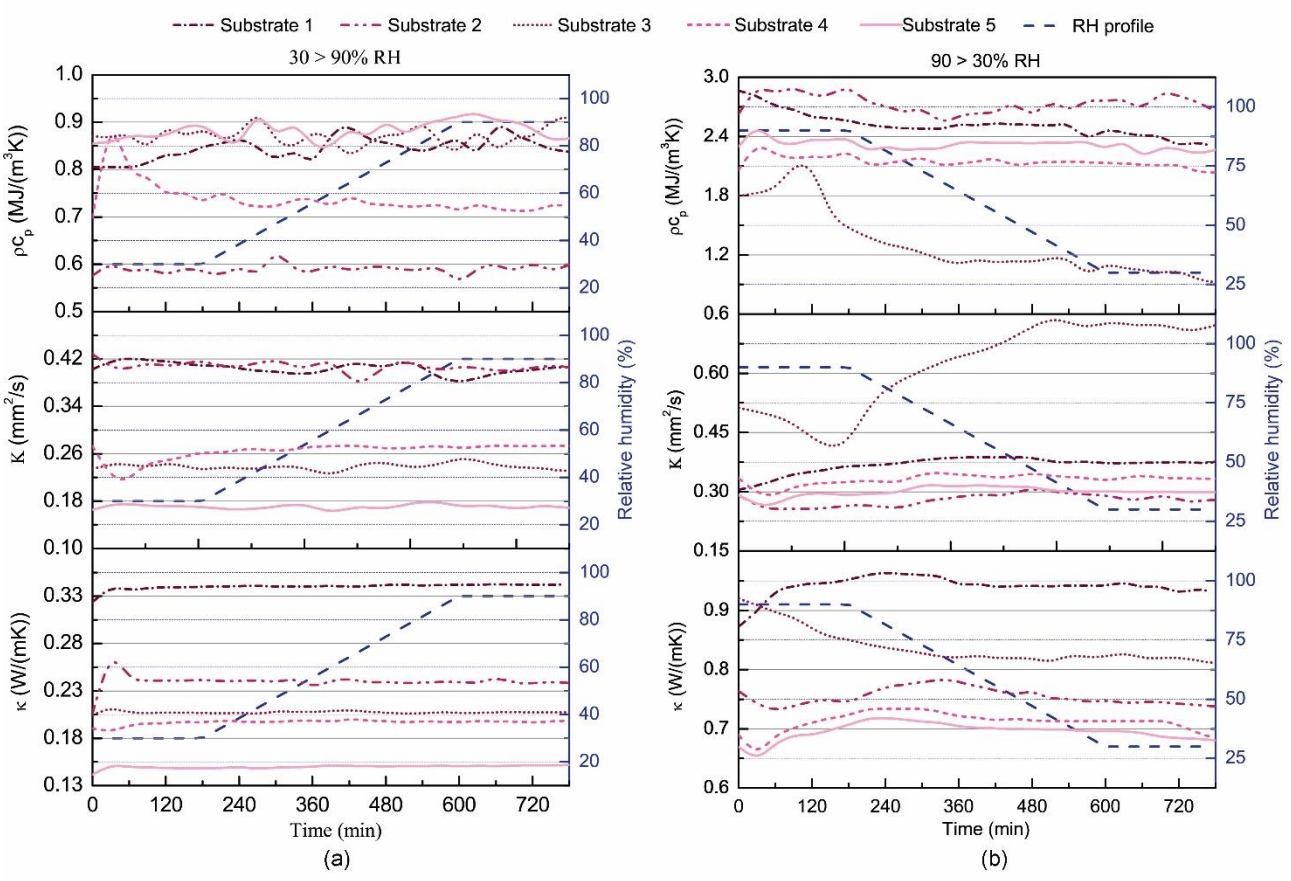

Figure 5. Dynamic hygrothermal analysis with varying RH values: (a) from 30% to 90%, at 21°C, and (b) from 90% to 30%, at 21°C.

A completely different behavior, however, can be detected when cycle (iii) is considered (Figure 5b). In this case, in fact, all samples are characterized by highly different thermal properties when compared to the previous cycles, as a consequence of the huge amount of absorbed water through the rain simulation procedure. During the cycle all the considered samples, with the exception of Substrate 3, registered a slight increase in thermal conductivity and diffusivity, and a specular reduction in volumetric specific heat. Such peculiar behavior, generally, is greater than the experimental error (see Figure 7) and can be associated to the water percolation phenomenon, which occurs quite slowly within the inner matrix of the denser substrates.

Substrate 3 sample, on the other hand, experiences a pseudo-logarithmic thermal conductivity reduction during the course of the cycle, while the values of diffusivity and volumetric specific heat, show an inflection point after about 2 hours from the beginning of the hygrothermal forcing, and then logarithmically increase and reduce, respectively. In this case, in fact, the substrate is characterized by a much smaller density value, thus offering a reduced resistance the motion of water.

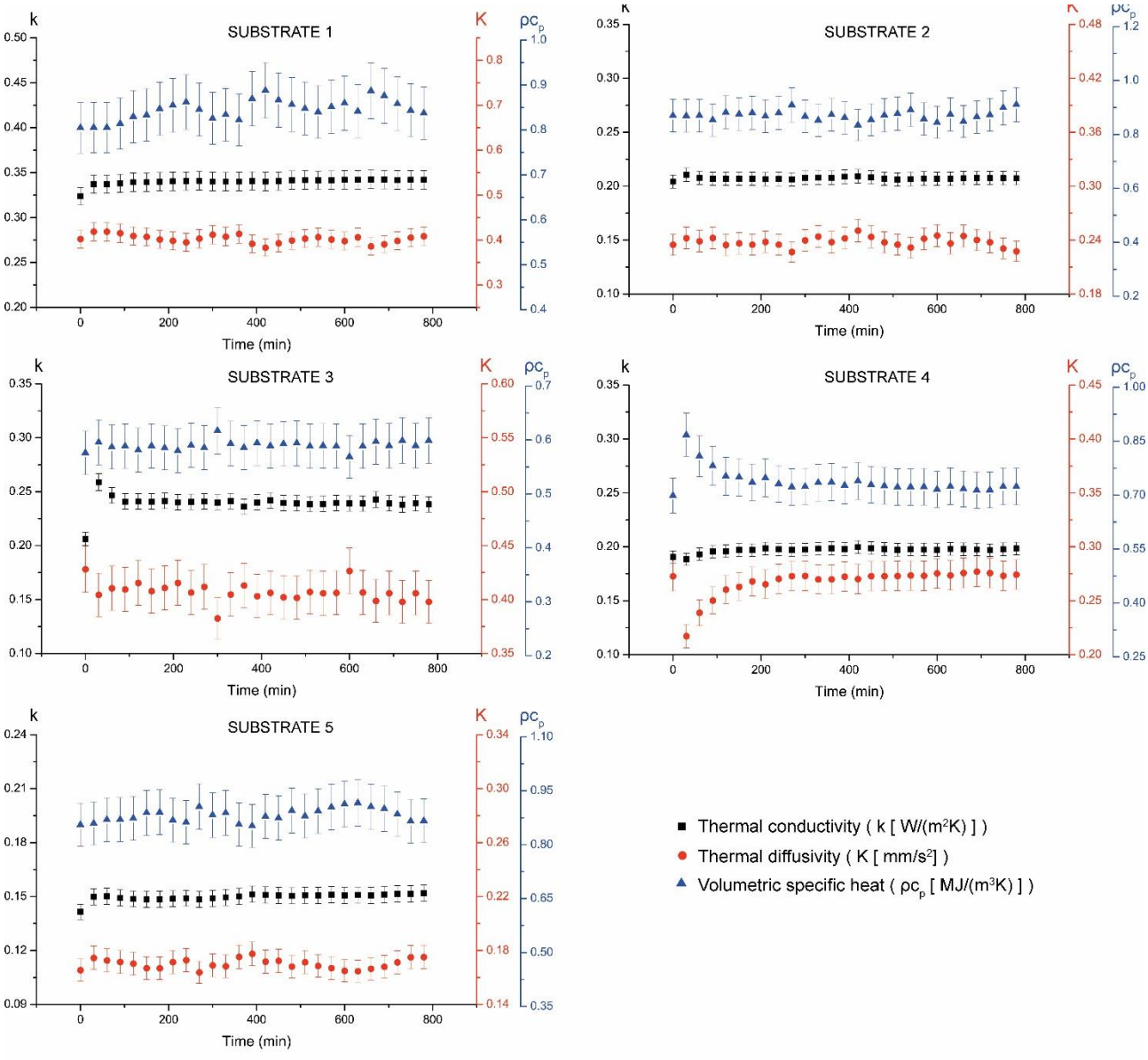

Figure 6. Dynamic hygrothermal analysis with varying RH values, i.e. from 30% to 90%, at 21°C, considering the instrumental error associated to each measurement of the profiles.

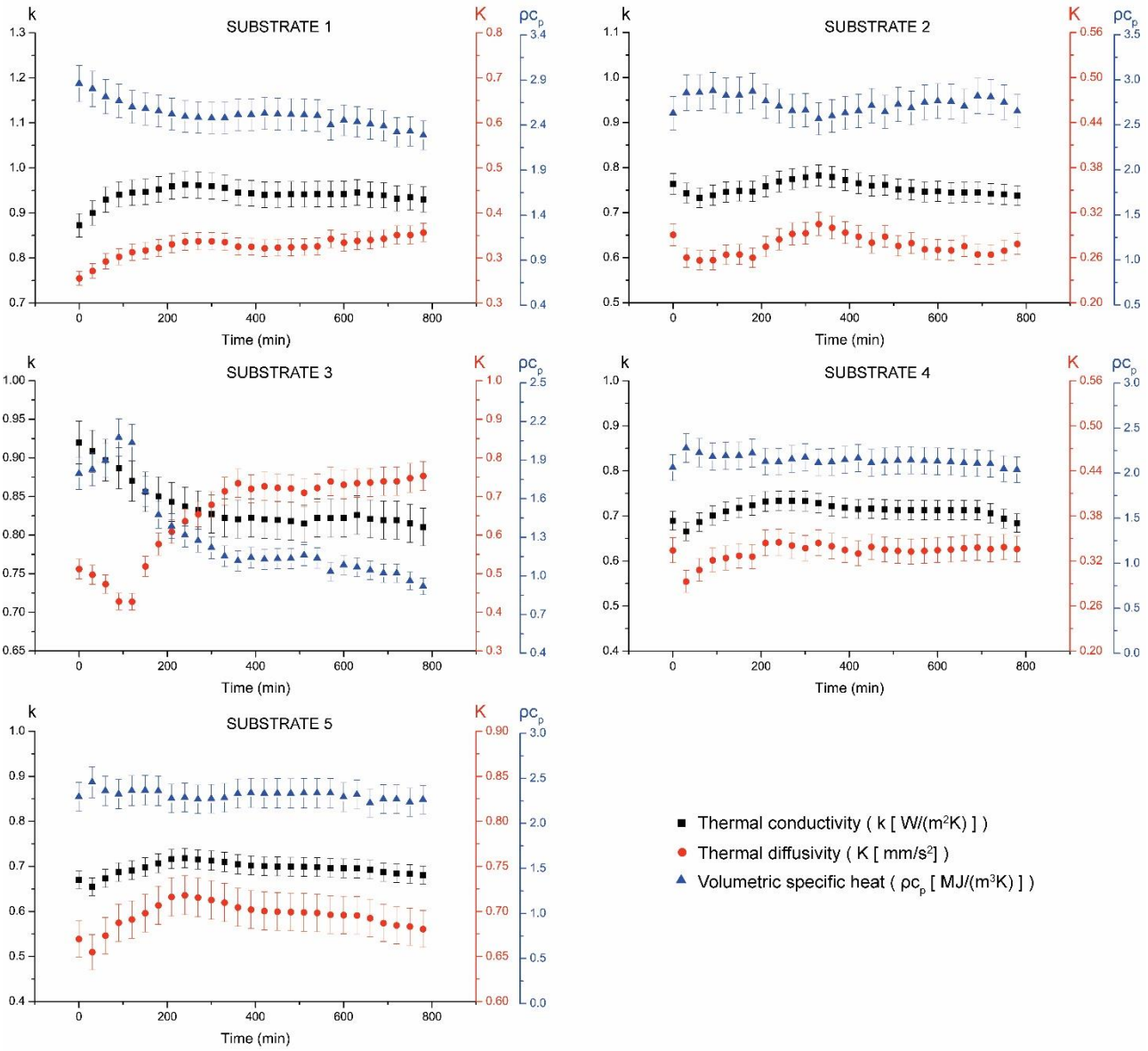

Figure 7. Dynamic hygrothermal analysis with varying RH values, i.e. from 90% to 30%, at 21°C, considering the instrumental error associated to each measurement of the profiles.

4.2. Results from the acoustic characterization

Figure 8 presents the sound absorption trend at 10%, 30% and 90% RH, for every green roof substrate considered in this work. Results show that very-dry substrates, i.e. those at 10% RH, are generally associated to better acoustic absorption properties, if compared to those with higher water contents, i.e. 30% and 90% RH. In particular, at 10% RH the 20 mm thick samples of substrate 3, 4 and 5 show the highest absorption peaks in the medium-low frequencies of the spectrum, reaching 0.92, 0.99 and 0.93 at 1896, 1912 and 1672 Hz, respectively. However, when the 30 and 90% RH conditions are considered, the same samples behave better at higher frequencies (in range 5128-6396 Hz) where they reach α values of 0.64, 0.51 and 0.78, and 0.62, 0.42 and 0.77, respectively (see Table 3).

Furthermore, increasing material densities generally causes lower acoustic absorption capability. In fact, every specimen produced by using the highest density material, i.e. substrate 1, is always associated with the worst absorption performance when compared to similar configurations of the other samples. In the same way, increasing sample thicknesses, and consequently higher sample densities due to higher compaction caused by the own weight of the substrate, usually deteriorate the absorption trend of the samples, particularly in the case of dry substrates (see Table 3).

This is due to the morphological characteristics of the investigated materials. The selected green roof substrates can, indeed, be considered as porous absorbers, since they owe their good acoustic performance to friction and thermal losses taking place at the boundary layer between the solid frame of the substrate and the interstitial fluid. Consequently, the absorption capability of the samples is directly related to the amount of open porosities within the inner matrix of the substrates [38]. In this view, denser and more compact materials are inevitably associated to lower acoustic absorption properties.

Additionally, as expected, in the low frequency region, the acoustic absorption performance of every investigated configuration varies as a function of the sample thickness. More in detail, by taking a closer look at Figure 8, it can be noticed that increasing sample thicknesses always shift the main absorption peak of the substrates towards lower frequencies, while also reducing its average amplitude and width. This is because, when porous absorbers are taken into account, thicker layers are generally needed to effectively damp the incident sound wave in this frequency region.

Concerning the effect of water content of the absorption performance of the samples, Figure 8 clearly shows that higher RH values significantly reduce the capability of the samples to dissipate the incident acoustic energy. This is probably because in higher RH conditions, the open cavities of the porous matrix are increasingly filled by water molecules, causing a much lower penetration depth of the sound wave in the absorber, and consequently, lower interaction at the interface between the different phases in the substrate.

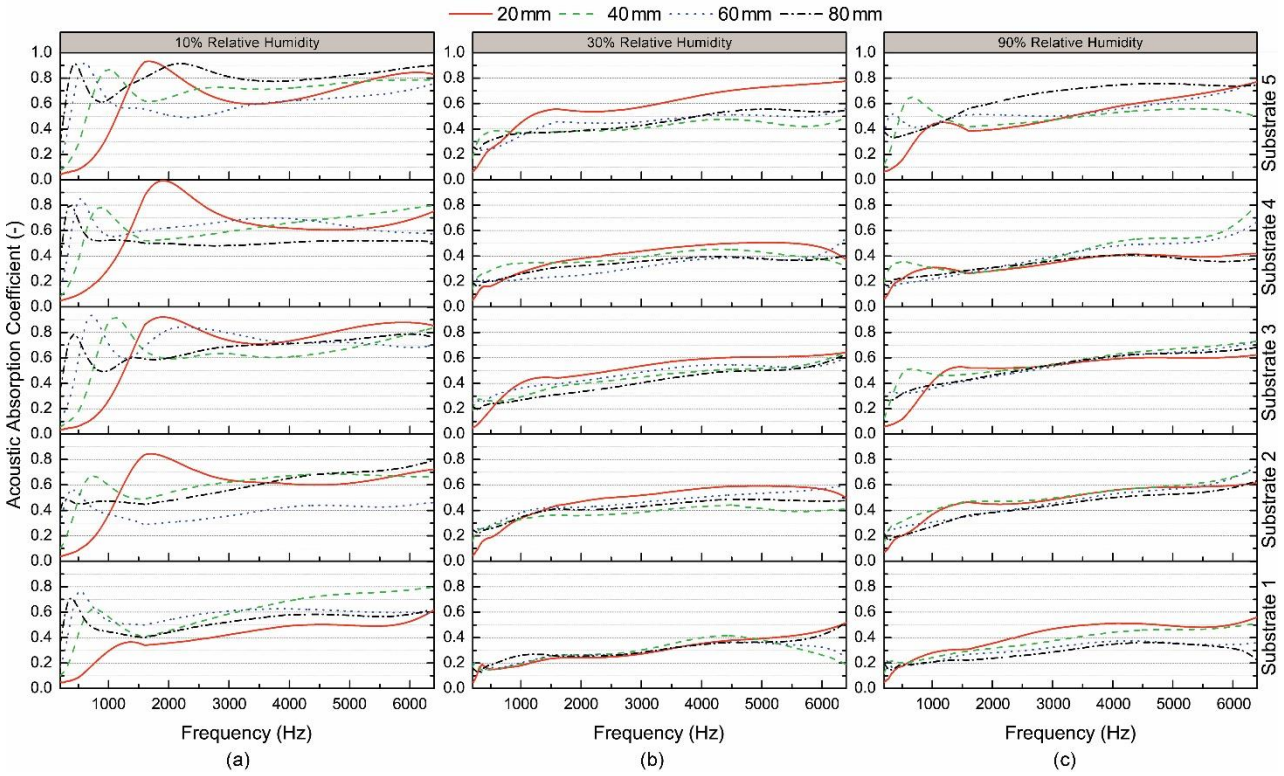

Figure 8. Acoustic absorption coefficient at 21°C, for (a) 10%, (b) 30%, and (c) 90% RH.

Table 3. Peak acoustic absorption value (α_{MAX}) and specific wavelength where it is registered ($\lambda_{\alpha MAX}$) for each investigated sample.

		Cycle (i)		Cycle (ii)		Cycle (iii)	
	Thickness (mm)	**α_{MAX} (%)**	**$\lambda_{\alpha MAX}$ (Hz)**	**α_{MAX} (%)**	**$\lambda_{\alpha MAX}$ (Hz)**	**α_{MAX} (%)**	**$\lambda_{\alpha MAX}$ (Hz)**
Substrate 1	20	0.62	6384	0.52	6392	0.56	6396
	40	0.80	6392	0.41	4424	0.51	6398
	60	0.78	532	0.37	4544	0.37	4240
	80	0.71	372	0.52	6384	0.36	4544
Substrate 2	20	0.85	1688	0.59	5024	0.62	6384
	40	0.96	4704	0.44	4488	0.73	6384
	60	0.56	410	0.60	6384	0.75	6384
	80	0.79	6396	0.49	4584	0.63	6392
Substrate 3	20	0.92	1896	0.64	6392	0.62	6390
	40	0.92	1104	0.65	6392	0.73	6384
	60	0.93	726	0.60	6384	0.73	6396
	80	0.79	6016	063	6396	0.68	6384
Substrate 4	20	0.99	1912	0.51	5128	0.42	6336
	40	0.80	864	0.45	4232	0.79	6384
	60	0.85	532	0.54	6396	0.66	6384
	80	0.81	366	0.40	6392	0.41	4296
Substrate 5	20	0.93	1672	0.78	6392	0.77	6396
	40	0.87	1000	0.49	6384	0.65	656
	60	0.92	608	0.56	6392	0.77	6384
	80	0.92	2184	0.56	5024	0.76	4704

As regards the acoustic insulation performance of the samples, the obtained results in terms of transmission loss (TL) are plotted in Figure 9, Figure 10 and Figure 11 for the configuration with 10%, 30% and 90% RH, respectively. In this case, every TL trend is separately presented, e.g. Figure 9.a and Figure 9.b, because the acoustic analyses carried out by using the large (200-1600 Hz) and the small (1600-6400 Hz) tube

configuration do not perfectly match in the shared frequencies region. This is probably due to the serious boundary effects which can easily take place in the small configuration, when ununiform specimen constituted by bug particles compared to the total diameter of the tube, such as the green roof substrates investigated in this work, are taken into account. Consequently, these results should not be considered as absolute values to be compared with those obtained in a diffuse field (using ISO 10140-2 standard [42]), however they still provide useful information about comparative analysis between the different investigated configurations.

More in detail, by comparing the insulation capability of the samples in the frequency range 100-1600 Hz, investigated by using the large tube configuration, every substrate shows increasing insulation properties, with increasing sample thicknesses. This desirable phenomenon is not always verified when the small configuration is considered, due to the main geometrical properties of the samples and of the experimental setup. Furthermore, in the range 100-1600 Hz, all the samples, with the exception of the 20 mm thick one, follow a mass law-like insulation pattern, and their slope increases with increasing thicknesses for every substrate.

Finally, the effect of water content looks different in the large and the small tube configuration. More in detail, for frequencies below 1600 Hz, the very-dry samples, i.e. with an RH value equal to 10%, always present the lowest insulation trend, with the resonance-driven region confined below the frequency of 200 Hz. On the other hand, the insulation capability of every considered sample significantly enhances for thicknesses above 20 mm, when both the 30% and the 90% RH configurations are considered. In these cases, however, the resonance region shows to be comparatively larger, since every sample presents a resonance peak around 500 Hz. This is due to the different effect produced by the water molecules on the different grain sizes dispersed in the substrates matrix. In any case, such particular effect produces similar pattern for the 30% and the 90% RH configuration, even though when the 90% RH one is taken into account, the additional resonance peak is always shifted towards higher frequencies (see Figure 12). In the middle-high frequencies, on the other hand, no huge differences can be detected among the different configurations.

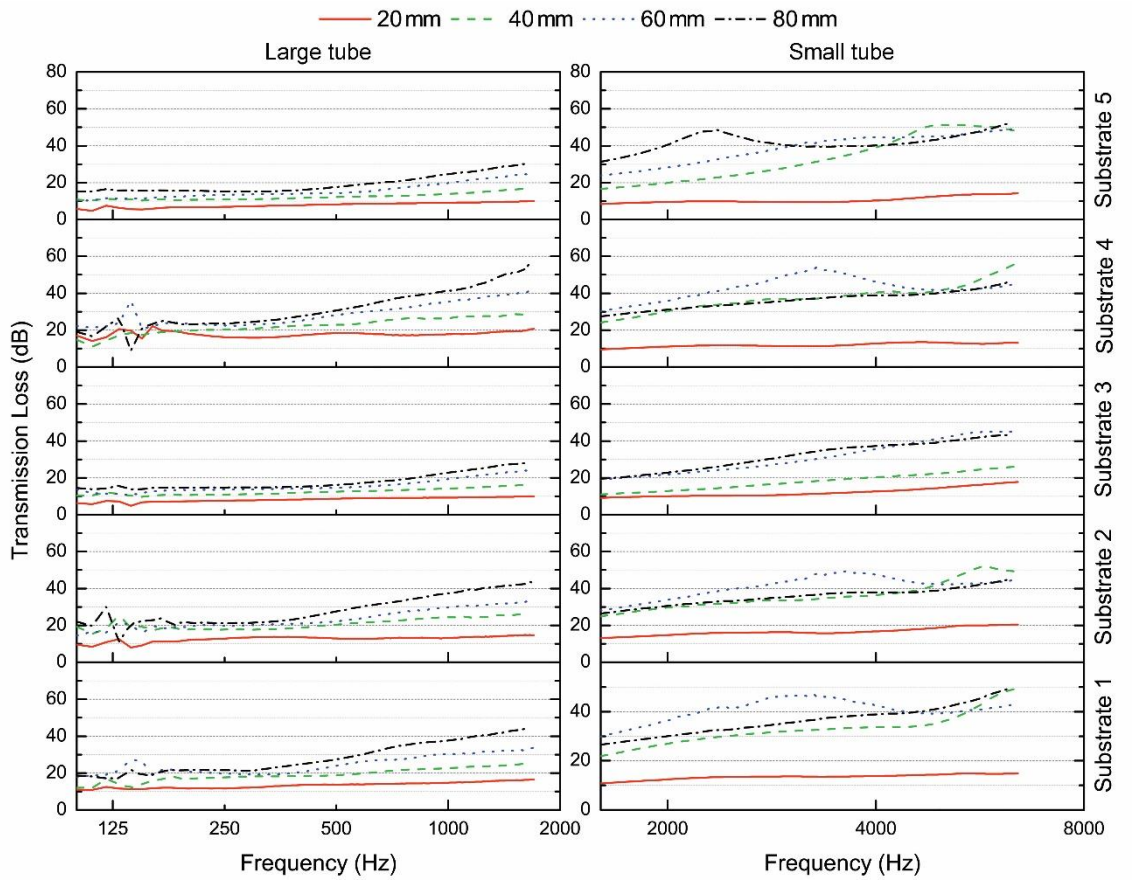

Figure 9. Acoustic transmission loss at 21°C and 10% RH, for the 5 selected green roof substrates.

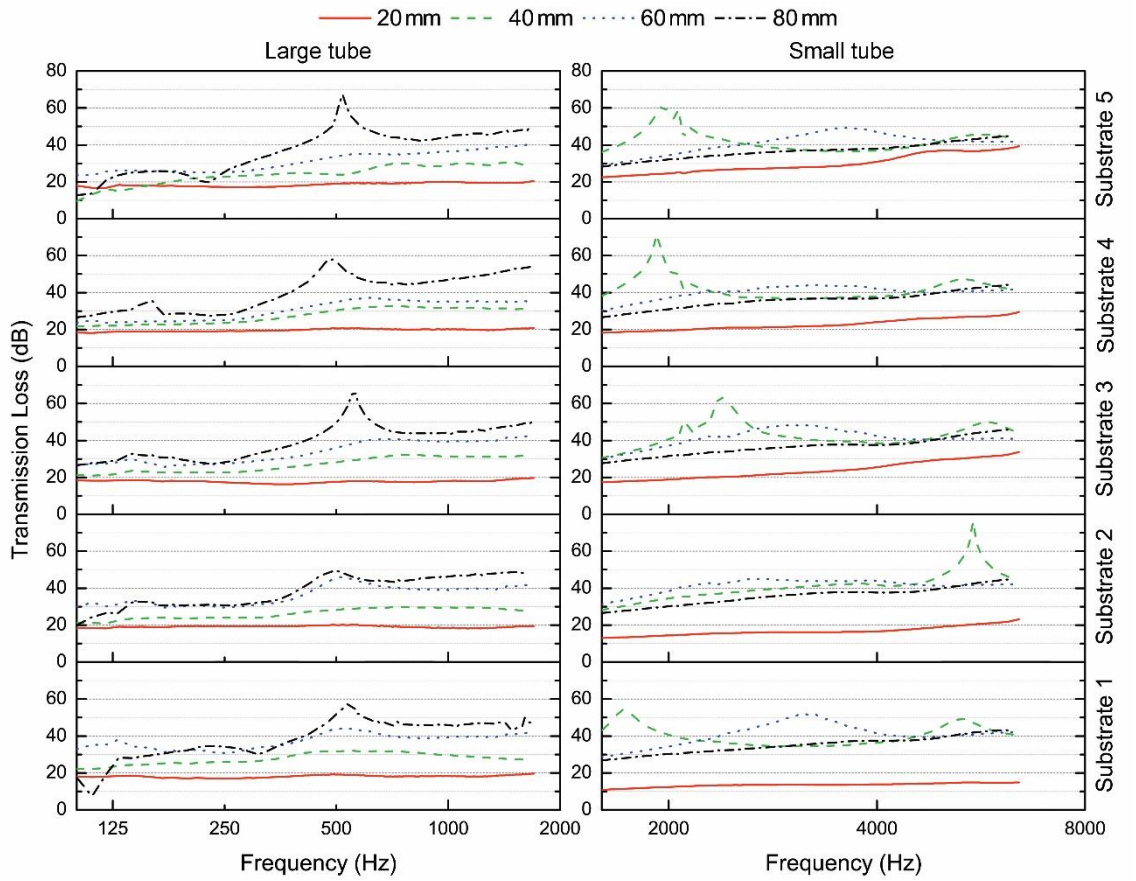

Figure 10. Acoustic transmission loss at 21°C and 30% RH, for the 5 selected green roof substrates.

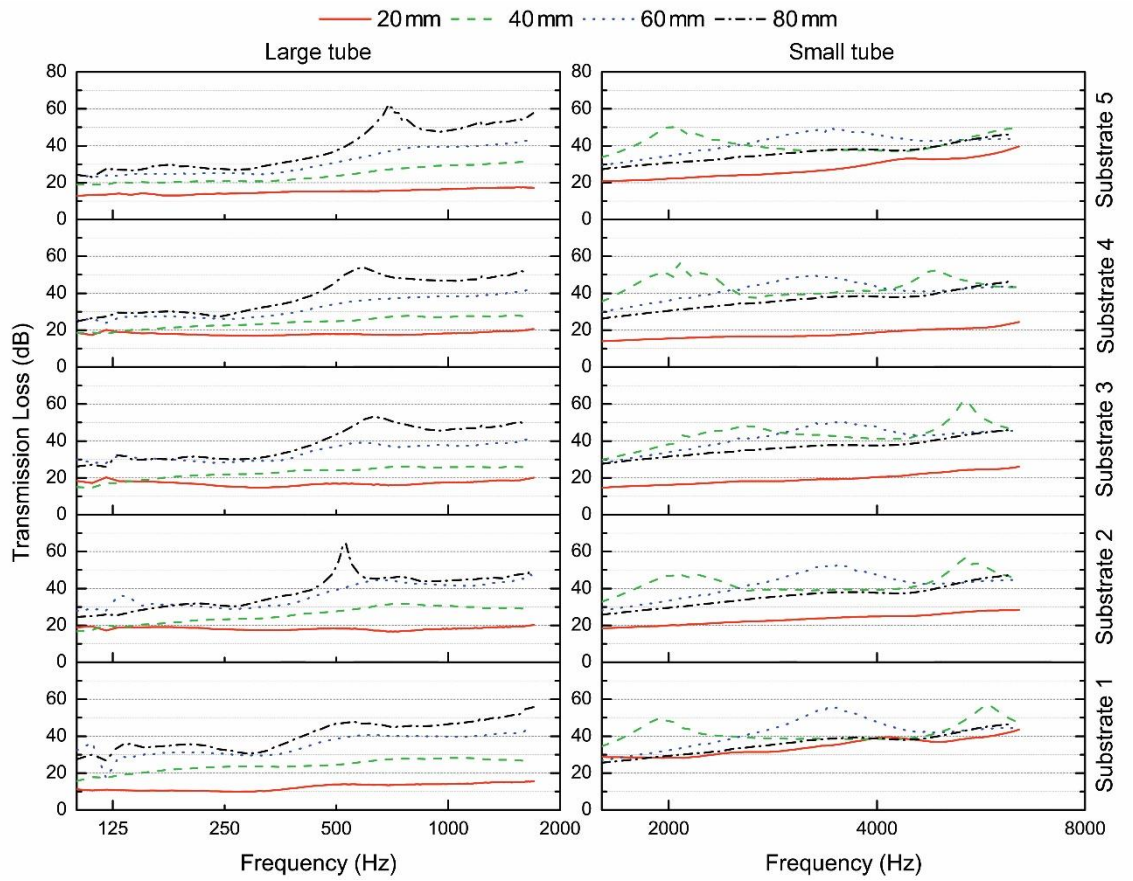

Figure 11. Acoustic transmission loss at 21°C and 30% RH, for the 5 selected green roof substrates.

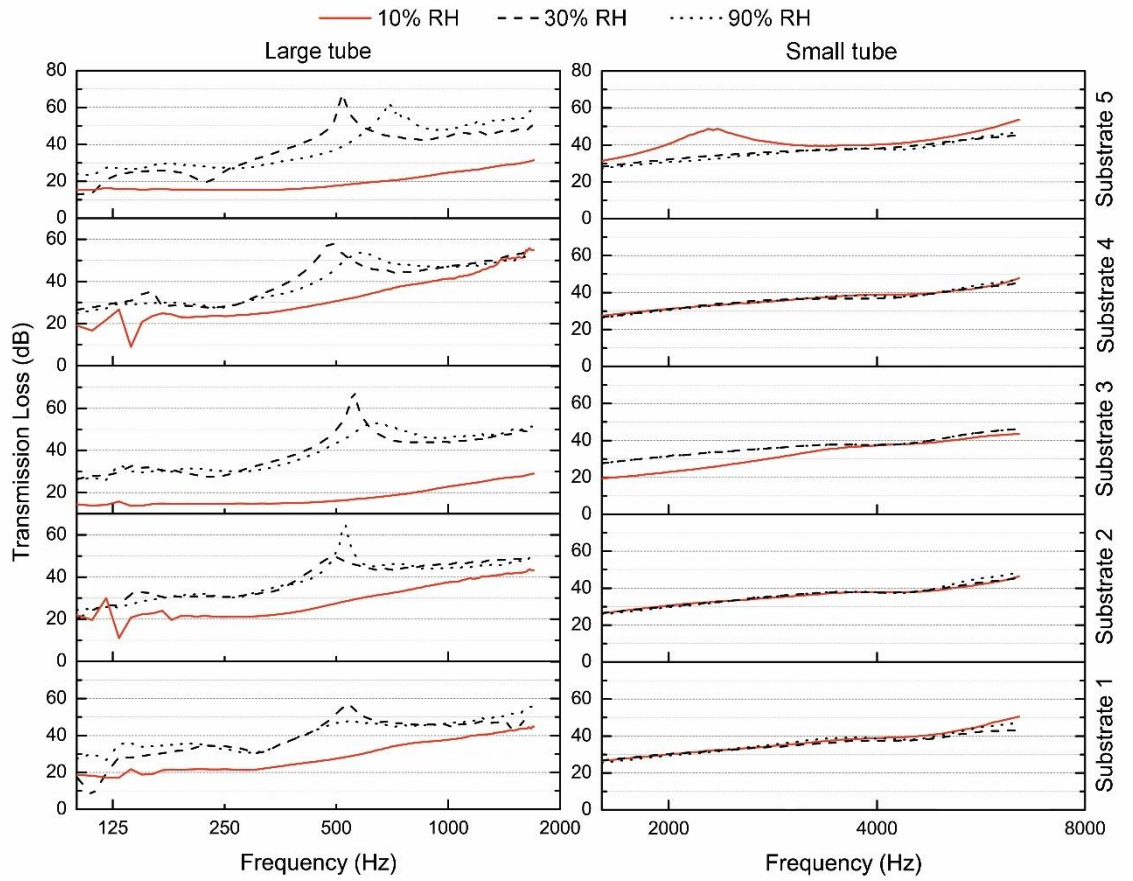

Figure 12. Acoustic transmission loss at 21°C, for 80 mm thick green roof substrates samples, at three different RH values: 10%, 30%, and 90%.

5. Conclusions

In this work, the thermal and acoustic behavior of five substrates for green roof applications were investigated under a daily realistic basis, with changing the final water content of the system. More in detail, real meteorological data from a weather station located in Perugia (Italy) characterizing the day with the highest oscillation in relative humidity in the period January 1st – July 31st 2017 were selected and used to test the samples within the controlled environment of a climatic chamber. Therefore, thermal and acoustic analyses were conducted on the substrates by means of the Hot Disk 2500S and the Brüel & Kjær 4260 impedance tube to investigate the diurnal oscillations of their performance.

In particular, the transient plane source method was repeatedly applied during the conditioning procedure to assess the thermal performance variation of the engineered green roof substrates in terms of thermal conductivity, thermal diffusivity and volumetric specific heat. Additionally, the acoustic absorption and insulation capability of the samples were also investigated, as a function of water content, by carrying out an impedance analysis using stationary plane waves at 10, 30 and 90% RH.

Results from the thermal analyses showed that in very-dry conditions, i.e. 10% RH, the values of thermal conductivities and diffusivities are inversely correlated to the organic content of the mixture. The volumetric specific heat, on the other hand, was mostly affected by the density of the considered samples. Additionally, during the humidification process that increased the environmental relative humidity from 30% to 90%, no significant variations were produced on the final value of the investigated properties, probably because of the relatively short duration of the cycle itself, i.e. about 13 hours. The experimental monitoring of the selected thermal properties carried out after a simulated raining process, on the other hand, showed a huge difference between the thermal performance of the investigated substrates, mostly because of the different impact of water percolation as a function of the composites density, and organic content.

The acoustic measurements also demonstrated that the samples with the lowest RH content present the highest sound absorption capability, and that substrates characterized by lower density values, i.e. substrate 3 and 5, always show the best damping behavior, due to the higher amount of interconnected open porosities in their matrix. Additionally, no huge differences were detected among the 30% and the 90% RH configurations, probably because a small amount of water in the superficial cavities is enough to highly reduce the sound wave penetration depth within the absorber matrix. As for the acoustic insulation analysis, results showed that for frequencies below 1600 Hz, the 10% RH samples, always present the lowest insulation trend, and every resonance phenomenon is always confined below the frequency of 200 Hz. Finally, the acoustic transmission loss was highly affected by the RH content in the range 10-30%, where increasing water contents lead to better insulation trends, while the RH conditioning at higher levels, i.e. 90% RH, produced a limited effect on the final insulation capability of the samples.

All this considered, it can be stated that no single solution exists to maximize the thermo-acoustic performance of green roofs' application. On the contrary, the present study demonstrates the importance of considering several factors during the designing phase of vegetated solutions for building applications, such as specific local climatic conditions, substrates' density, thickness and overall organic content.

As a future development of this study, it could be interesting to evaluate the effect of long term humidification processes and extend the acoustic analyses to simulated rain processes. Furthermore, it could be very interesting to also investigate the thermo-acoustic behavior of the substrates in real scale applications, eventually using real green roof stratigraphy and installations.

Acknowledgements

Acknowledgments are due to the "CIRIAF program for UNESCO" in the framework of the UNESCO Chair "Water Resources Management and Culture". The research leading to these results has received funding from the European Union's Horizon 2020 research and innovation program under grant agreement No. 657466 (INPATH-TES). The work is also partially funded by COOL CRETE Project, under the framework of Call L. 598/94 Art. 11 – Industrial research and experimental development (Energy sector) supported by Luigi Metelli S.p.A., and by the Spanish government ENE2015-64117-C5-1-R (MINECO/FEDER) in collaboration with the company Buresinnova S.A (Mercabarna Flor - Local n. 412 Ctra. Antiga de València, 1. 08830 Sant Boi de Llobregat. www.buresinnova.com). The authors would like to thank the Catalan Government for the quality accreditation given to their research group (2017 SGR 1537). GREA is certified agent TECNIO in the category of technology developers from the Government of Catalonia. Julià Coma would like to thank Ministerio de Economia y Competitividad de España for Grant Juan de la Cierva, FJCI-2016-30345.

References

[1] Directive 2010/31/eu of the European Parliament and of the Council of 19May 2010 on the energy performance of buildings (recast). Available from: http://www.epbd-ca.eu.

[2] D'Ambrosio Alfano FR, Dell'Isola M, Ficco G, Tassini F. Experimental analysis of air tightness in Mediterranean buildings using the fan pressurization method. Build Environ 2012;53;16-25.

[3] Gasparella A, Pernigotto G, Baratieri M, Baggio P. Thermal dynamic transfer properties of the opaque envelope: Analytical and numerical tools for the assessment of the response to summer outdoor conditions. Energ Buildings 2011;43-9;2509-2517.

[4] Lešić V, Martinčević A, Vašak M. Modular energy cost optimization for buildings with integrated microgrid. Appl Energy 2017;197;14-28.

[5] Pisello AL, Castaldo VL, Pignatta G, Cotana F, Santamouris M. Experimental in-lab and in-field analysis of waterproof membranes for cool roof application and urban heat island mitigation. Energ Buildings 2016;114;180-190.

[6] Rosso F, Pisello AL, Cotana F, Ferrero M. Integrated Thermal-Energy Analysis of Innovative Translucent White Marble for Building Envelope Application. Sustainability 2014;6(8);5439-5462.

[7] D'Agostino D, Cuniberti B, Bertoldi P. Energy consumption and efficiency technology measures in European non-residential buildings. Energ Buildings 2017;153;72-86.

[8] Djedjig R, Belarbi R, Bozonnet E. Experimental study of green walls impacts on buildings in summer and winter under an oceanic climate. Energy and Buildings; 2017;150;403-411.

[9] Serra V, Bianco L, Candelari E, Giordano R, Montacchini E, Tedesco S, Larcher F, Schiavi A. A novel vertical greenery module system for building envelopes: The results and outcomes of a multidisciplinary research project. Energy and Buildings 2017;146;333-352.

[10] GhaffarianHoseini AH, Dahlan ND, Berardi U, GhaffarianHoseini A, Makaremi N, GhaffarianHoseini M, Sustainable energy performances of green buildings: A review of current theories, implementations and challenges. Renew Sust Energ Rev 2013;25;1-17.

[11] Coutts AM, Daly E, Beringer J, Tapper NJ. Assessing practical measures to reduce urban heat: Green and cool roofs, Build Environ 2013;70;266-276.

[12] Blank L, Vasl A, Levy S, Grant G, Kadas G, Dafni A, Blaustein L. Directions in green roof research: A bibliometric study, Build Environ 2013;66;23-28.

[13] Ouldboukhitine S-E, Belarbi R, Sailor DJ. Experimental and numerical investigation of urban street canyons to evaluate the impact of green roof inside and outside buildings. Appl Energy 2014;114:273-282.

[14] Ascione F, Bianco N, de' Rossi F, Turni G, Vanoli GP. Green roofs in European climates. Are effective solutions for the energy savings in air-conditioning? Appl Energy 2013;104:845-859.

[15] NiachouA, Papakonstantinou K, Santamouris M, Tsangrassoulis A, Mihalakakou G. Analysis of the green roof thermal properties and investigation of its energy performance. Energ Buildings 2001;33(7);719-729.

[16] Metselaar K. Water retention and evapotranspiration of green roofs and possible natural vegetation types. Resour Conserv Recy 2012;64;49-55.

[17] Coma J, de Gracia A, Chàfer M, Pérez G, Cabeza LF. Thermal characterization of different substrates under dried conditions for extensive green roofs. Energ Buildings 2017;144;175-180.

[18] Kosareo L, Ries R, Comparative environmental life cycle assessment of green roofs. Build Environ 2007;42(7);2606-2613.

[19] Pérez G, Coma J, Barreneche C, de Gracia A, Urrestarazu M, Burés S, Cabeza LF. Acoustic insulation capacity of Vertical Greenery Systems for buildings. Appl Acoust 2016;110;218-226.

[20] Azkorra Z, Pérez G, Coma J, Cabeza LF, Bures S, Álvaro JE, Erkoreka A, Urrestarazu M. Evaluation of green walls as a passive acoustic insulation system for buildings. Appl Acoust 2015;89;46-56.

[21] Pérez G, Vila A, Rincón L, Solé C, Cabeza LF. Use of rubber crumbs as drainage layer in green roofs as potential energy improvement material. Appl Energy 2012;97:347-354.

[22] Connelly M, Hodgson M. Experimental investigation of the sound absorption characteristics of vegetated roofs. Build Environ. 2015;92;335-346.

[23] Connelly M, Hodgson M. Experimental investigation of the sound transmission of vegetated roofs. Appl Acoust 2013;74(10),1136-1143.

[24] Chemisana D, Lamnatou C. Photovoltaic-green roofs: An experimental evaluation of system performance. Appl Energ 2014;119;246-256.

[25] Jim CY. Air-conditioning energy consumption due to green roofs with different building thermal insulation. Appl Energ 2014;128;49-59.

[26] Pisello AL, Piselli C, Cotana, F. Thermal-physics and energy performance of an innovative green roof system: The Cool-Green Roof. Sol Energ 2015;116;337-356.

[27] Pérez G, Coma J, Cabeza LF, Green roofs and green facades for energy savings in buildings. Green Building and Phase Change Materials: Characteristics. Energy Implications and Environmental Impacts 2015;19–70.

[28] Coma J, Pérez G, Solé C, Castell A, Cabeza L.F. Thermal assessment of extensive green roofs as passive tool for energy savings in buildings. Renew Energ 2016;85;1106-1115.

[29] Verstraeten WW, Veroustraete F, Feyen J. Assessment of Evapotranspiration and Soil Moisture Content Across Different Scales of Observation. Sensors (Basel, Switzerland). 2008;8(1):70-117.

[30] Van Renterghem T, Botteldooren D. Influence of rainfall on the noise shielding by a green roof. Build Environ 2014;82;1-8.

[31] Payá J, Corberán JM, de Gracia A, Castell A, Cabeza LF. Thermal characterization of buildings from the monitoring of the AC system consumption. Energ Buildings 2016;116;59-68.

[32] Navarro L, de Gracia A, Niall D, Castell A, Browne M, McCormack SJ, Griffiths P, Cabeza LF. Thermal energy storage in building integrated thermal systems: A review. Part 2. Integration as passive system. Renew Energ 2016;85;1334-1356.

[33] Nidal H, Randall C. Soil thermal conductivity Effects of density, moisture, salt concentration and organic matter, Soil Sci Soc Am 2000;64;1285–1290.

[34] Zhang T, Cai G, Liu S, Puppala AJ. Investigation on thermal characteristics and prediction models of soils. Int J Heat Mass Transfer 2017;106;1074–1086.

[35] SS-EN ISO 22007-2:2015. Plastics – Determination of thermal conductivity and diffusivity – Part 2: Transient plane source (hot disk) method, International Organization for Standardization (ISO), Geneva, Switzerland, 2015.

[36] Gustaffson SE. Transient plane source techniques for thermal conductivity and thermal diffusivity measurements of solid materials. Rev Sci INstrum 1991; 62:797-804.

[37] International Organization for Standardization, ISO 10534-2: Acoustics - Determination of Sound Absorption Coefficient and Impedance in Impedance Tubes - Part 2: Transfer-function Method 1998.

[38] Asdrubali F, Pisello AL, D'Alessandro F, Bianchi F, Fabiani C, Cornicchia M, Rotili A. Experimental and numerical characterization of innovative cardboard based panels: Thermal and acoustic performance analysis and life cycle assessment. Build Environ 2016;95;145-159.

[39] Pispola G, Horoshenkov KV, Asdrubali F. Transmission loss measurement of consolidated granular media. J Acoust Soc Am 2005;117(5);2716-2719.

[40] A. Vaz Sá, M. Azenha, H. de Sousa, A. Samagaio. Thermal enhancement of plastering mortars with Phase Change Materials: Experimental and numerical approach. Energ Buildings 2012;49;16-27.

[41] UNI EN ISO 6946. Building components and building elements - Thermal resistance and thermal transmittance - Calculation methods. International Organization for Standardization (ISO), Geneva, Switzerland, 2017.

[42] International Organization for Standardization, ISO 10140-2: Acoustics - laboratory Measurement of Sound Insulation of Building Elements - Part 2: Measurement of Airborne Sound Insulation, 2010.